Journal of Structural Biology **131,** 67–78 (2000) doi:10.1006/jsbi.2000.4260, available online at http://www.idealibrary.com on IDEAL

The Otoconia of the Guinea Pig Utricle: Internal Structure, Surface Exposure, and Interactions with the Filament Matrix

Ulysses Lins,*,† Marcos Farina,‡ Maurı´cio Kurc,* Gavin Riordan,* Ruediger Thalmann,§ Isolde Thalmann,§ and Bechara Kachar*,[1]

**Section on Structural Cell Biology, National Institute on Deafness and Other Communication Disorders, NIH, Bethesda, Maryland 20892-4163; †Departamento de Microbiologia Geral and ‡Departamento de Anatomia, Universidade Federal do Rio de Janeiro, Rio de Janeiro 21941-590, Brazil; and §Department of Otolaryngology, Washington University School of Medicine, St. Louis, Missouri 63110*

Received November 30, 1999, and in revised form March 6, 2000

A unique feature of the vertebrate gravity receptor organs, the saccule and utricle, is the mass of biomineral structures, the otoconia, overlying a gelatinous matrix also called "otoconial membrane" on the surface of the sensory epithelium. In mammals, otoconia are deposits of calcium carbonate in the form of composite calcite crystals. We used quick-freezing, deep etching to examine the otoconial mass of the guinea pig utricle. The deep-etching step exposed large expanses of intact and fractured otoconia, showing the fine structure and relationship between their internal crystal structure, their surface components, and the filament matrix in which they are embedded. Each otoconium has a compact central core meshwork of filaments and a composite outer shell of ordered crystallites and macromolecular aggregates. A distinct network of 20-nm beaded filaments covers the surface of the otoconia. The otoconia are interconnected and secured to the gelatinous matrix by surface adhesion and by confinement within a loose interotoconial filament matrix. The gelatinous matrix is a dense network made of yet another type of filament, 22 nm in diameter, which are cross-linked by shorter filaments, characteristically 11 nm in diameter. Our freeze-etching data provide a structural framework for considering the molecular nature of the components of the otoconial complex, their mechanical properties, and the degree of biological versus chemical control of otoconia biosynthesis.

© 2000 Academic Press

Key Words: **otoconia; otoconial membrane; otoliths; otolithic membrane; utricle; mechanosensory transduction; vestibular system; biomineralization.**

INTRODUCTION

The vestibular system in mammals consists of three semicircular canals, the saccule, and the utricle. The canals respond to angular acceleration, whereas the saccule and the utricle respond to linear acceleration. The saccular and utricular sensory epithelia are covered by an accessory extracellular superstructure that contains a large mass of calcium carbonate composite crystals, the otoconia, to make the macular receptors more sensitive to linear acceleration (Lim, 1984; Ross *et al.,* 1987). The otoconial mass is made of thousands of otoconia, averaging 10 mm in length, that overlay a gelatinous matrix often called "otoconial membrane" (Lim, 1984). The gelatinous matrix has two layers. Its upper layer is a dense isotropic network of filaments to which the otoconial mass is attached (Kachar *et al.,* 1990). Its lower layer consists of columnar filaments that hold the gelatinous membrane at a specified distance above the surface of the sensory epithelium (Kachar *et al.,* 1990). The sensitivity of the utricle and saccule to acceleration is due to the high density and specific gravity of the otoconia. When the body experiences linear acceleration, the otoconia undergo a differential inertial movement with respect to the surrounding viscoelastic fluid-bathed matrix. A precise description of how the otoconia are integrated within the otoconial membrane is important for understanding how the inertia of the otoconia is transmitted through this viscoelastic matrix to effectively stimulate the sensory stereocilia.

[1] To whom correspondence should be addressed at Section on Structural Cell Biology, NIDCD, National Institutes of Health, Bldg. 36, Rm. 5D-15, Bethesda, MD, 20892-4163. Fax: (301) 4021765. E-mail: kacharb@nidcd.nih.gov.

Otoconia consist of microcrystals joined together by organic matrices to form composite crystals. Calcium carbonate crystals form the mineral phase of most otoconia, but exceptions exist (Carlstro¨m, 1963). Aragonite is the most common calcium carbonate found in fish, although calcite, vaterite, and calcium carbonate monohydrate are also present (Calstro¨m, 1963; Gauldie, 1993; Oliveira *et al.*, 1996). Amphibians have two types of otoconia. In the utricle, the otoconia are calcite polymorphs, whereas in the saccule, both prismatic and pinacoid shaped aragonitic otoconia are present (Marmo *et al.*, 1983; Pote and Ross, 1991; Steyger *et al.*, 1995). Mammals have calcite otoconia that are barrel-shaped, with triplanar faceted ends (Lim, 1984).

The organic phase of otoconia consists of several proteins, including a major glycoprotein species, otoconin, which accounts for .90% of the total protein (Pote and Ross, 1986; Ornitz *et al.*, 1998). It appears that each crystal polymorph is associated with a unique otoconin. Calcitic otoconia contain otoconin-90 (Wang *et al.*, 1998), and aragonitic otoconia contain otoconin-22 (Pote *et al.*, 1993a), suggesting that the otoconins influence the type of crystal polymorph formed.

Understanding the molecular organization of the composite structure of the otoconia is important for understanding their biophysical properties and their rate of growth and stabilization. The coexistence of hard crystals and slender filaments makes this complex matrix difficult to analyze by conventional microscopy. Attempts to study the internal architecture of otoconia and the relationship between their organic and mineral components have been hindered by artifacts, produced by chemical etching solutions used to partially or entirely dissolve the hard mineral component. A number of investigators have described an organic core with peripherally radiating fibrillar structures in sections of decalcified mammalian calcitic otoconia (Lim, 1984; Pote and Ross, 1986; Steyger and Wiederhold, 1995). The electron microscopic appearance of these organic structures varied widely, depending on the preparatory procedures.

Because of the procedures involved and the characteristics of the specimen preparation required, these techniques also do not provide a resolution sufficient to visualize the structural relationships between the otoconial surface and the loose network of extracellular filaments that adhere to it. In a previous report on the amphibian saccular macula (Kurc *et al.*, 1999), we described novel aspects of the structure and surface topography of the aragonitic otoconia, using the quick-freezing deep-etching replica technique. We now have used the freeze-etching technique to examine the otoconial mass of the guinea pig utricular maculae. We provide a detailed morphology of the internal structure of the calcitic otoconia and describe distinct filament networks in the otoconia core and on their surface. Due to the regular shape and smooth surface of the otoconia and to the resolution of our technique, we observed with unprecedented detail the substructure of the filaments, how the filaments interact with the inorganic crystalline structure, and how they connect the otoconia into an integrated otoconial mass.

67 1047-8477/00 $35.00
Copyright © 2000 by Academic Press All rights of reproduction in any form reserved.

MATERIAL AND METHODS

Six adult pigmented guinea pigs, 300 to 400 g, were anesthetized with carbon dioxide and decapitated. The animals were treated in accordance with the NIH guidelines for the care and use of laboratory animals. The temporal bones were promptly removed, immersed in 2% glutaraldehyde in phosphate-buffered saline (pH 7.4) for 1 h, and transferred to distilled water. The macula of the utricle was dissected with care to preserve the attachment of the otoconial membrane to the sensory epithelium. After several gentle washes in distilled water, each macula was placed onto a 400-mm-thick slice of Bacto-agar (Difco Laboratories, Detroit, MI) and mounted on filter paper glued to an aluminum specimen holder. The specimen was quick-frozen by contact with a liquid nitrogen-cooled sapphire block of a Life Cell CF-100 quick-freezing machine (Research and Manufacturing Co., Tucson, AR) and promptly transferred to liquid nitrogen. The specimens were fractured at 2150°C in a Balzers BAF301 freezefracture apparatus, etched for 10 min at 2100°C, and rotary shadowed with platinum at a 15° angle and with carbon at a 90° angle. Organic material was cleaned in hypochlorite bleach and the inorganic phase dissolved with 5% hydrochloric acid. Replicas were observed and photographed on a Zeiss 902 or Zeiss 912 transmission electron microscope in zero-loss imaging mode.

RESULTS

The Supporting Gelatinous Matrix

To visualize the structure of the supporting gelatinous matrix or "otoconial membrane" (Lim, 1984), we gently removed a portion of the overlying otoconia from the surface of the finely dissected utricular macula by blowing fluid from a pipette. Thus we could maintain several layers of otoconia and the upper portion of the gelatinous matrix within the 20 mm of optimal tissue preservation (vitreous freezing) allowed by the quick-freezing technique (Heuser *et al.*, 1979). Figure 1 shows the deep-etching view of a plane of fracture through the supporting gelatinous layer. The layer consists of a cross-linked, isotropic three-dimensional meshwork of filaments (Fig. 1a). The filaments often presented a beaded appearance. The diameter of the filaments at the beaded regions was 22 6 0.4 nm (N 5 20) (Fig. 1b, arrows). Figure 1b also shows that these filaments are occasionally cross-linked by thinner filaments 11 6 0.4 nm in diameter (N 5 20) (arrowheads). The mesh size of the smaller cavities in the matrix ranges from 60 to 200 nm. In addition to small cavities, large cavities

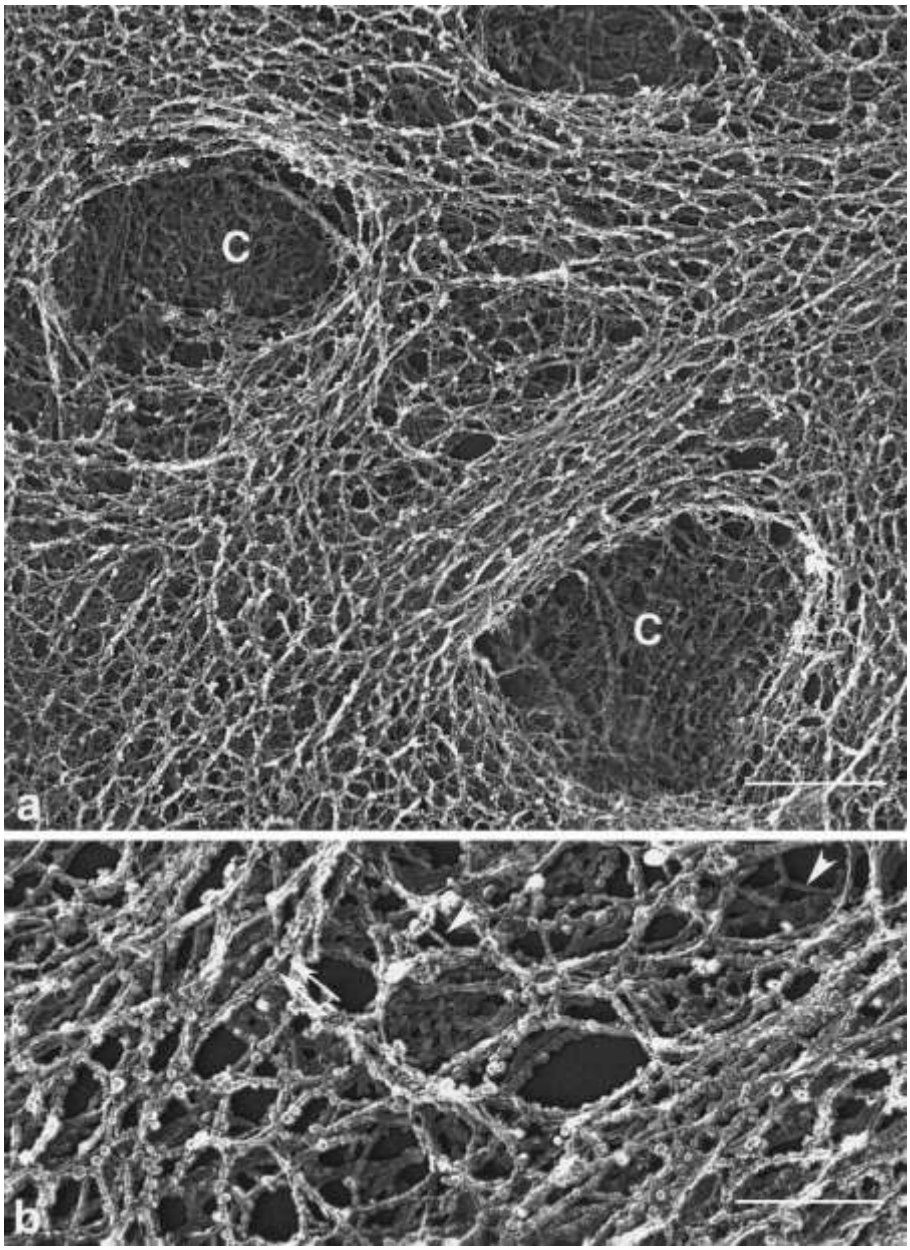

FIG. 1. Deep-etching views of the supporting gelatinous layer. (a) The layer consists of a cross-linked, isotropic three-dimensional meshwork of filaments that delimit small and large cavities (C). Higher magnification (b) shows that the filaments have a beaded substructure (arrows) and are cross-linked by thinner filaments (arrowheads). (a) Bar, 0.5 mm; (b) bar, 0.2 mm.

(.0.5 mm) are present and correspond to the cavities which are frequently observed in the central or striolar region of the supporting gelatinous matrix or "otoconial membrane" (Lim, 1984).

Interotoconial Filament Matrix

Deep-etching views of fractures above the gelatinous matrix and through the otoconial mass show numerous, barrel-shaped, otoconia with characteristic triplanar faceted ends embedded in a loose filament matrix (Fig. 2a). These filaments measured 24 6 2.1 nm in diameter (N 5 20) and were attached laterally to, or ended on, the surface of the otoconia (Fig. 2b, arrows), appearing to intervene between the otoconia to collect them into a loose assemblage. Because of the freeze-fracture and deep etching, the filaments of the interotoconial matrix that were severed by the fracture knife recoiled dur-

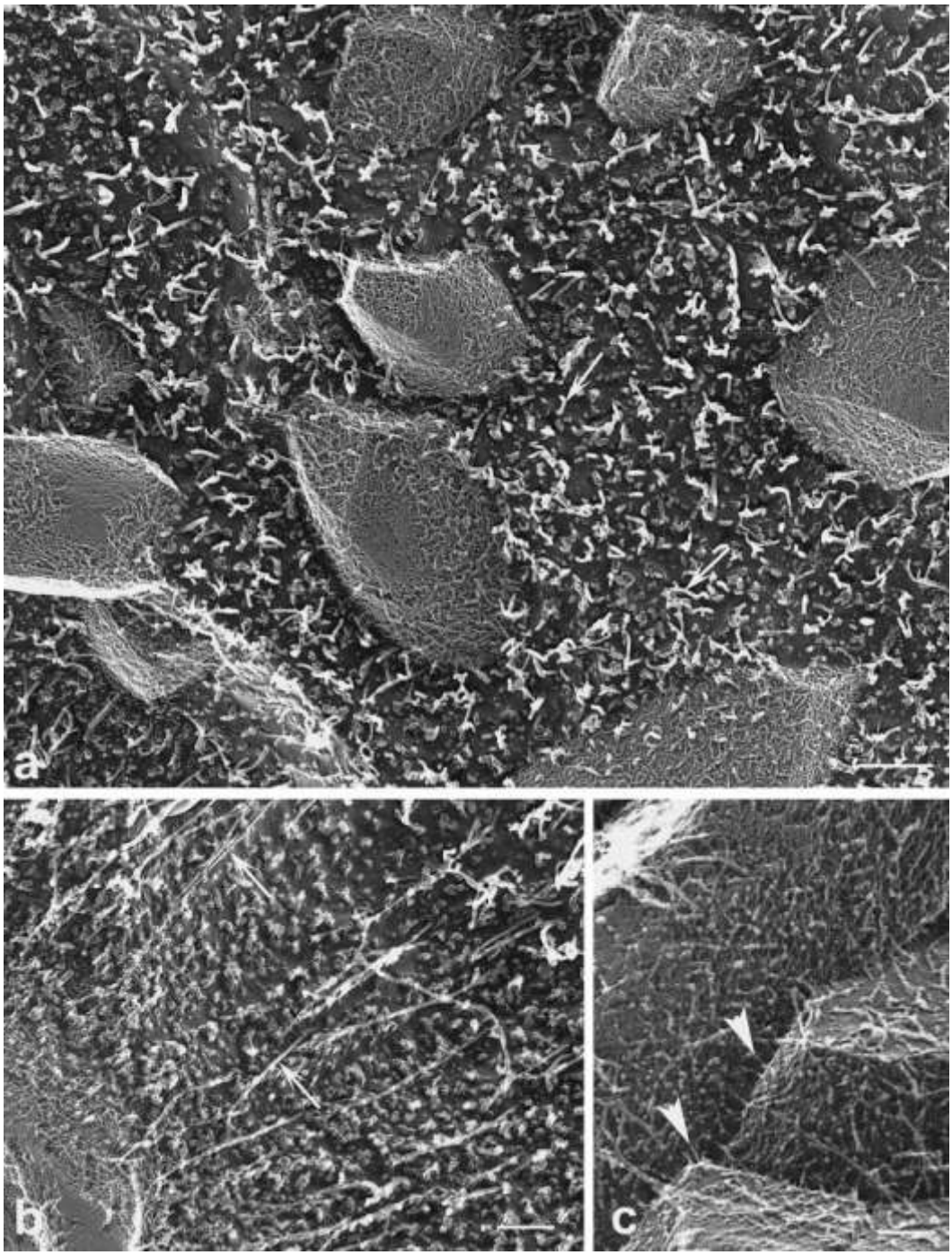

FIG. 2. Deep-etching views of fractures through the otoconial mass. (a) View shows numerous, barrel-shaped otoconia embedded in a loose filament matrix. Many of the filaments appear severed and recoiled from the freeze-fracture and deep-etch procedure (arrows); (b) filaments (arrows) attach laterally or end on the surface of the otoconia; (c) Three adjacent otoconia appear to be linked to one another by filament cross-links (arrowheads). (a) Bar, 1.0 mm; (b) bar, 0.5 mm; (c) bar, 0.25 mm.

ing etching of the embedding ice (Fig. 2a, arrows). *Otoconia Surface* Some otoconia also appear to adhere to one another by the cross-linking of filaments present on their Because of the geometric shape of the otoconia, surface (Fig. 2c, arrowheads). the deep etching often exposes surfaces that form steep angles with the horizontal plane of fracture and the platinum/carbon rotary shadowing. Viewing of the projected images of these sharp angled surfaces in the transmission electron microscope is also complicated, because they have different orientations in relation to the incident angle of the electron beam. Therefore, we performed our morphological analyses on selected areas, in which the surface was close to the horizontal plane and optimal in relation of the rotary shadowing and viewing of the replicas (Fig. 3). We observed that a network of meandering filaments covers the lateral and rhombohedral surfaces of the otoconia. These meandering filaments can be several micrometers long and bend across the sharp edges of the otoconia surface (Fig. 3b). Because the otoconial surface is flat and relatively smooth, it provides an excellent background for viewing the surface filaments. Individual filaments and details of their substructure are clearly resolvable (Fig. 3b, inset). Our images are reminiscent of images of molecular structures produced by the freeze-etching mica sheet technique (Heuser, 1983). The filaments have a "beaded" substructure and the diameter of the bead units is 20 6 0.6 nm (N 5 20). The center to center spacing between bead units in the filament is 26 6 3.4 nm (N 5 20). The network of meandering filaments appears at different densities, giving the otoconia surface a mosaic appearance. We also observed 20-nm globular particles scattered on the surface between the filaments (Fig. 3a, arrows). These particles appear to be similar to the "beads" that make up the filaments and may correspond to monomers of the filaments. Thin filaments (5.6 6 0.2 nm, N 5 20) radiate laterally from the beaded filaments (Fig. 4a, arrowheads). When the beaded filaments with their lateral thin filaments are present at high density, they appear to form a two-dimensional lattice (Figs. 4a and 4b). During the fracture step, the knife occasionally grazes the surface of an otoconium and separates the filament network from the mineral surface, exposing the raw surface of the mineral matrix (Fig. 4a). Fortuitously, one of these separated networks was etched and replicated, showing in a side angle that the surface filaments can form a two-dimensional network (see inset in Fig. 4a).

Internal Structure of the Otoconia

The freeze-fracture often splits open the otoconia and with the deep-etching step the central core and the outer mineralized thick layer or shell can be directly observed in the replicas (Fig. 5). Otoconia of all sizes consistently show an organic core and a dense crystalline cortex. The transition between core and mineralized cortex is abrupt and the core occupies approximately one third to one half of the volume of the otoconium. The core is formed by a tight meshwork of filaments 14 6 0.6 nm in diameter (N 5 20) that differ from the surface filaments (Fig. 5). This tight meshwork has a mesh size of 32 6 2 nm (N 5 20), giving the central core a characteristic texture (Fig. 5b). The overall shape of the central core follows the basic contour of the otoconia (Fig. 5a, arrows) including their faceted terminal extensions typical of calcite crystals (Figs. 3a and 5a). Often, the transition between the network of filaments that form the central core and the solid composite mineralized structure of the outer shell, as shown in Fig. 5c, is strikingly sharp. At this interface, a regular array of short filaments radiates from the core matrix and ends perpendicularly to the inner surface of the mineral outer shell (Fig. 5c, arrows).

A variety of fracture patterns is observed in the outer shell of the freeze-fractured otoconia. Mostly these fracture faces show sharply contoured arrays of prismatic columns (Fig. 5b) or laminar structures (Fig. 6). The direction of the prismatic and laminar structures is most frequently perpendicular to the external surfaces (Figs. 5 and 6). However, the angles differ from region to region and abrupt changes in the organization of the columns occur near the rhombohedral terminations (Figs. 5a and 5b). Occasionally, surface artifacts are observed when the knife produces a cut surface instead of a fractured one. A cut and sheared surface can be distinguished by knife marks which are oriented in the direction of the knife motion (Fig. 5a). Often the fracture exposes extended flat areas of the laminar composite crystalline structure, where the smooth background of the crystallite surfaces reveals small irregular globular particles or aggregates likely to correspond to organic (proteins or glycoproteins) components (Fig. 6b, arrows). In several places, the fracture plane exposes deep radial grooves in the composite mineral layer, evidently corresponding to channels through the otoconia outer shell, connecting the central core with the surface of the otoconia (Fig. 4c, arrows). In fact, close examination of the surface of the otoconia shows pore-like openings that line up with the surface filaments (Fig. 4b). These pores are clearly visible in the smooth, "naked" surface of the otoconia (Fig. 4a), where the freeze-fracture knife removed the filaments. It is interesting to note that, aside from the pores, both the external (Fig. 4a) and the internal (Fig. 5c) surfaces of the composite mineralized layer of the otoconia are quite smooth or "polished," despite the fact that this layer is formed by aggregates of composite crystallites.

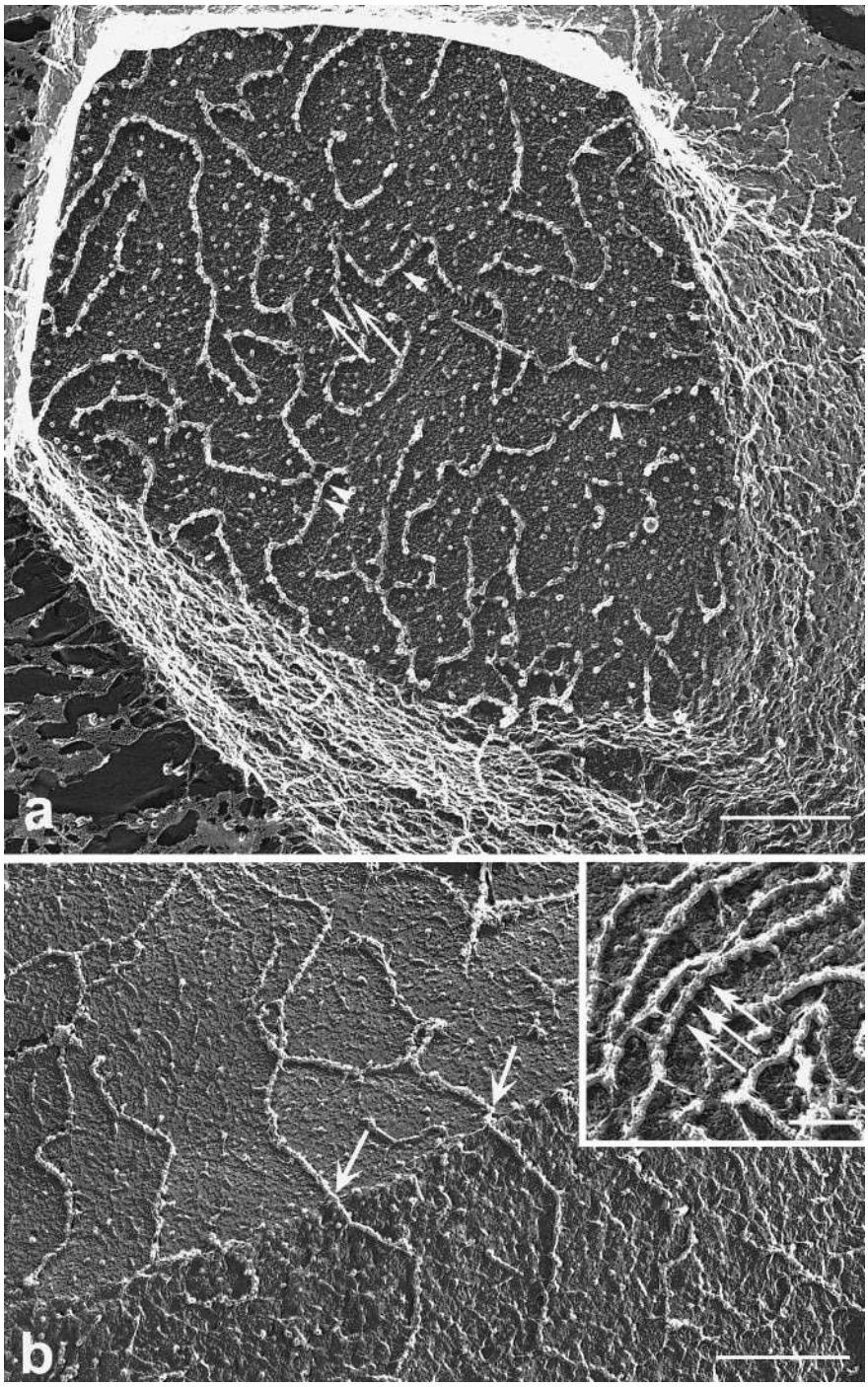

FIG. 3. Meandering filaments (arrowheads) and globular particles (arrows) cover the surfaces of the otoconia (a). (b) The filaments can be long and bend over the edges of the otoconia surface (arrows). Inset shows fine details of the filament's "beaded" structure (arrows). Bars, 0.5 mm.

DISCUSSION

sensory epithelia provide the basis for their special-

The mechanical qualities of the extracellular ac- ized mechanotransduction functions. The analysis of cessory structures on the surface of the vestibular their fine structure provides important information

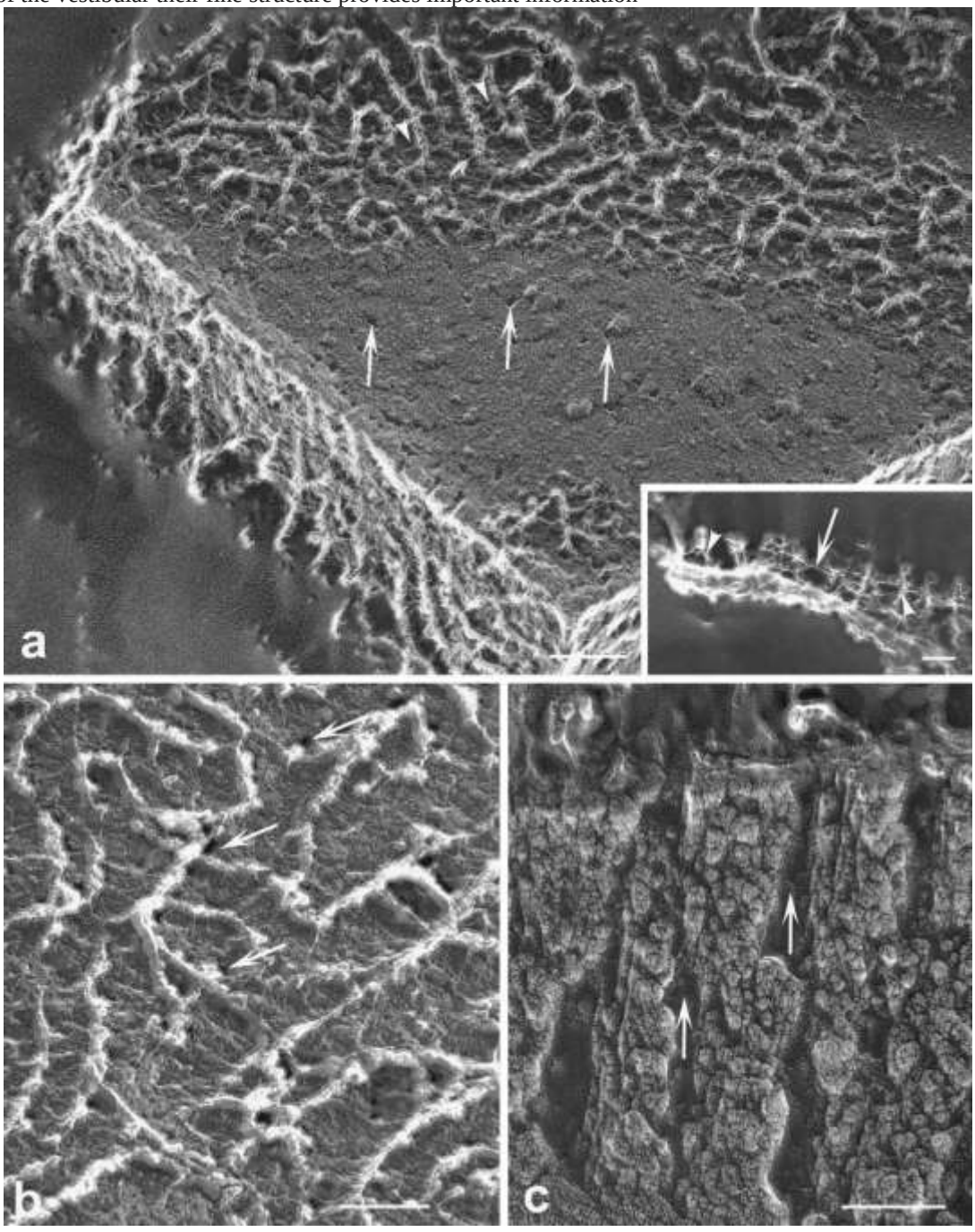

FIG. 4. Detailed view of the surface of the otoconia. (a) The exposed raw surface of the mineral matrix reveals pore-like openings (arrows). Thin filaments (arrowheads) radiate laterally from the beaded filaments. (Inset) Deep-etching view of a fortuitously patch of surface filaments shows thinner filaments (arrow) interconnecting the surface filaments (arrowheads). (b) The pore-like openings (arrows) appear near or under the surface filaments. (c) The fracture plane through the mineralized outer shell of this otoconium shows several deep radial channels (arrows) that seem to connect the central core with the otoconium's outer surface. (a) Bar, 0.2 mm; (b) bar, 0.1 mm; (c) bar, 0.2 mm. (Inset) Bar, 0.1 mm.

complementary to the often more difficult direct me- quick-freezing deep-etching technique to investigate chanical measurements and other physiological the fine structure and microarchitecture of the exstudies. In the present study we have used the tracellular matrix that covers the surface of the sen-

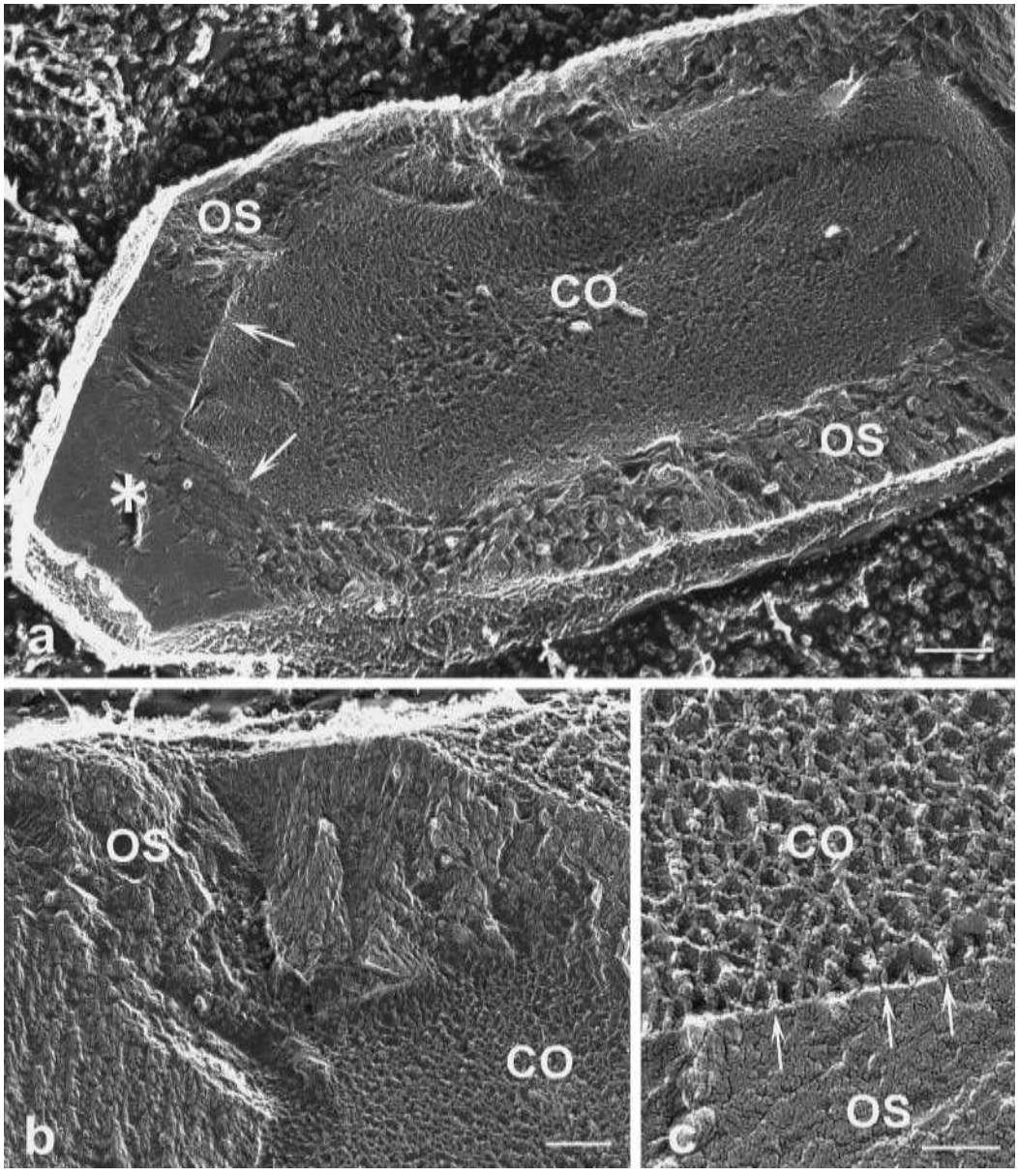

FIG. 5. Panoramic (a) and detailed (b and c) views of an otoconium, fractured in a plane parallel to its main axis, show an organic central core (CO) formed by a tight meshwork of filaments and a dense crystalline outer shell (OS). The outer shell shows different patterns of fracture. Occasionally the freeze-fracture knife shears the mineralized matrix, leaving knife marks on the surface (*). The transition between core and mineralized outer shell is abrupt and the interface between core and outer shell follows the basic contour of the otoconia, including their triplanar faceted ends (arrows in a). A closeup of the interface (c) shows short filaments (arrows) radiating in an orderly way from the core matrix (CO) and ending perpendicularly on the inner surface of the outer shell. (a) Bar, 0.5 mm; (b) bar,

0.2 mm; (c) bar, 0.1 mm.

sory epithelium of the guinea pig utricule. Several distinct networks of filaments support this complex extracellular matrix, containing the otoconia and bathed in endolymph, a fluid rich in K^1 and low in Na^1 and Ca^{21} (Salt *et al.*, 1989). The organization of, and structural relationships between, these networks are summarized in the diagram in Fig. 7.

The myriad of otoconia is contained as an integrated mass by a loose filament network observed in our freeze-etching images in the interotoconial spaces. The much lower rigidity of this matrix when compared with the supporting gelatin matrix, or otoconia membrane, can be inferred by the fact that it is easily disrupted, allowing the dispersion of the

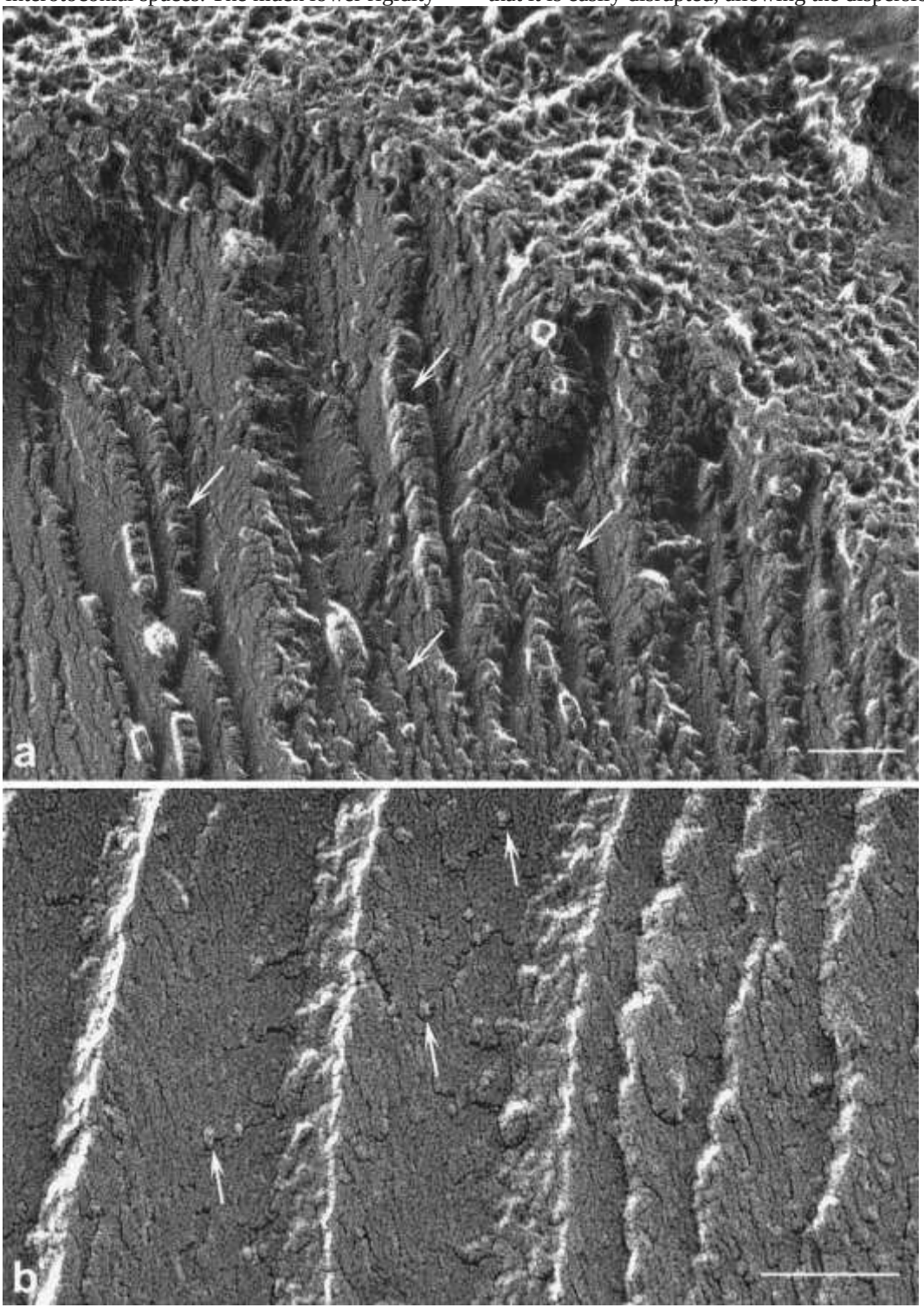

FIG. 6. Fracture faces of the otoconial outer shell mineral matrix. The fracture exposed laminar structures disposed perpendicularly to the otoconial external surface (arrows). In (b), globular particles (arrows), possibly proteins or glycoproteins, are present on the fracture faces of the laminar composite crystalline matrix. (a) Bar, 0.25 mm; (b) bar, 0.1 mm.

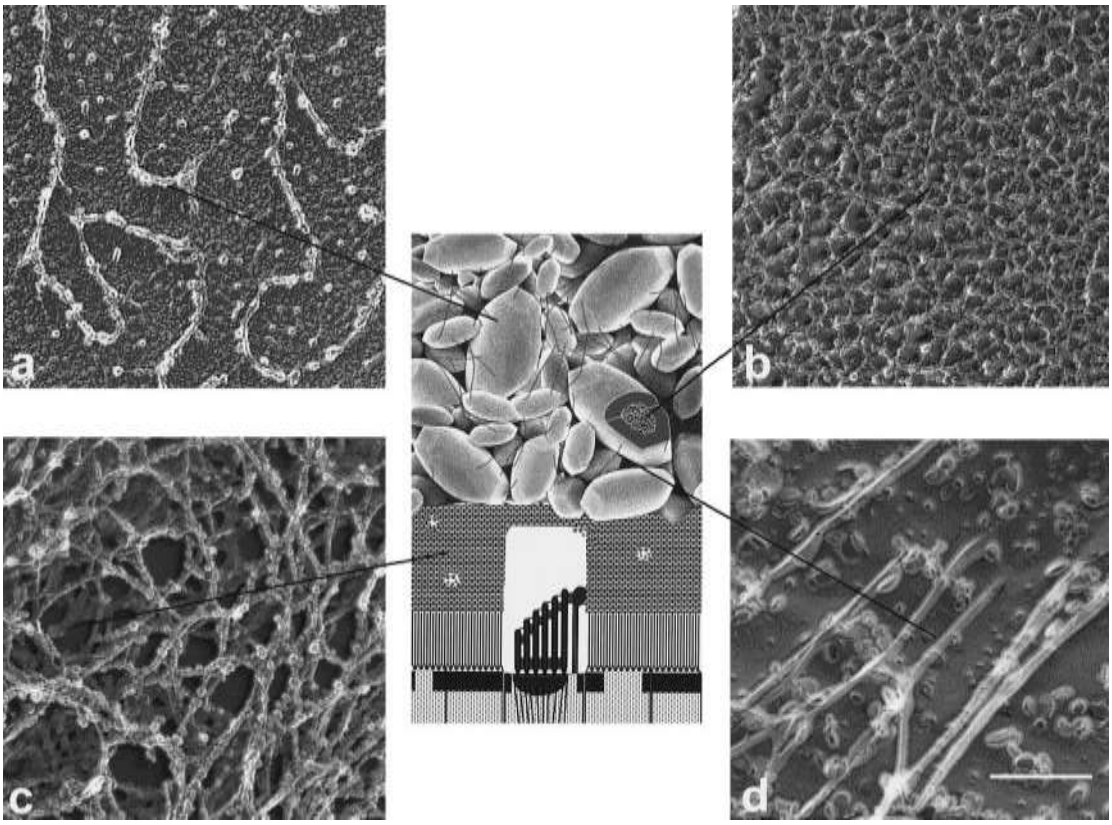

FIG. 7. Composite diagram summarizing our view of the organization of the filaments in the otoconial mass and gelatinous matrix. (a) A network of meandering beaded filaments covers the surface of the otoconia. (b) Internally, the otoconia contain a central core of densely organized filaments. (c) The supporting gelatinous matrix is in direct contact with the otoconial mass and consists of a cross-linked, isotropic three-dimensional network of filaments. (d) A loose filament network forms the inter-otoconial matrix. Bar, 0.2 mm.

otoconia even by a gentle fluid jet from a micropipette even after fixation of the tissue. In contrast, the supporting gelatin matrix resists the fluid jets used to disperse the otoconia and can be removed intact by peeling it from the surface of the unfixed epithelium with a pair of forceps (Howard and Hudspeth, 1987). The supporting gelatinous matrix must resist compressive forces and effectively transmit the force of inertia of the otoconial mass to the stereocilia bundle (Eatock *et al.,* 1987; Kachar *et al.,* 1990). The highly cross-linked isotropic texture of this layer strongly suggests that this matrix functions as a rigid plate and equally distributes the force of inertia of the many otoconia to all the stereocilia bundles (Kachar *et al.,* 1990). These filamentous structures in the gelatinous layer resemble those found in the tectorial membrane (Arima *et al.,* 1990). Whether they are biochemically similar or identical remains to be determined.

An important finding of our study is the network of meandering beaded filaments on the surface of the otoconia. The diameter, substructure, and network organization of these surface filaments is different from that of the otoconial core and from that of the interotoconial matrix and the supporting gelatinous matrix (Fig. 7). Nakai *et al.* (1996) used a low-vacuum SEM on unfixed and non-dehydrated specimens of the otoconial membrane. The authors described a 15- to 20-nm-thick layer of an amorphous substance on the surface of the otoconia. Our observations with freeze-etching replicas demonstrate that this layer, far from being amorphous, corresponds to a well-defined network of filaments. It is possible that in addition to a role in forming adhesive bonds between adjacent otoconia and in forming an integrated otoconial mass, these surface filaments may be involved in the shaping and turnover of the mineral components of the otoconia.

The outer layer or cortex of the calcitic otoconia has a composite crystallite organization. Previous studies on crushed otoconia by high-resolution TEM show an arrangement of small single crystallites with rounded edges and a fairly uniform diameter of about 100 nm (Mann *et al.*, 1983; Ross and Pote, 1984). Mann *et al.* (1983) concluded that otoconia represent a mosaic or composite of microcrystallites and organic matrix in which the crystallites form the basic building blocks of the structure. The otoconial cortex shows sharply contoured arrays of prismatic columns radiating toward the surface. The direction of the crystallite columns relative to the surface differed from region to region. The $CaCO_3$ in mammalian and avian otoconia form a calcite lattice, whereas in the amphibian and reptile sacculus the otoconia form an aragonite lattice. The predominant mineralization of the periphery of the calcitic otoconia may facilitate calcium turnover, contributing to otoconial maintenance and longevity (Ross and Pote, 1984; Fermin *et al.*, 1998). However, this attribute may also contribute to the onset of degenerative events, including decalcification and fragmentation of otoconia. Nevertheless, calcitic otoconial formation appears to have some potentially distinct advantages over aragonitic otoconial formation. Glycosaminoglycans/proteoglycans play a prominent inhibitory role in mineralization in various systems, and the conspicuous glycan component of otoconin-90 deserves consideration in this context (Wang *et al.*, 1998). Thus, available information suggests that otoconin-90, presumably in conjunction with other minor otoconins, directs the assembly and orientation of single crystallites into larger aggregates and limits excessive growth.

It can be assumed that most of the organic structures visible in the core of the calcitic otoconia represent the otoconial matrix protein otoconin-90, given that it accounts for more than 90% of the calcitic mammalian otoconia total protein (Pote and Ross, 1991; Wang *et al.*, 1998). Our results, showing that the filaments in the core of the otoconia are distinct from the filaments of the interotoconial matrix, also agree with recent biochemical data showing that otoconin-90 is present in the otoconia but not in the extraotoconial matrix (Ornitz *et al.*, 1998). Otoconin-90 has recently been cloned and found to contain two sequence domains closely resembling secretory phospholipase A_2 (Wang *et al.*, 1998). This is remarkable, considering that otoconin-22, the matrix protein of aragonitic amphibian otoconia, is also a homolog of phospholipase A_2, but in this case containing only a single sequence domain of that protein. The similarity between otoconin-90 and otoconin-22 suggests that calcitic and aragonitic otoconia share fundamental formation mechanisms.

Considering the limited size of otoconia and their precisely defined shape, the concomitant role of the matrix in limiting growth by controlled inhibition of mineralization becomes apparent. Mann *et al.* (1983) showed that there is no organic matter in the interior of the individual microcrystallites; however, they suggested that organic matter was present between the microcrystallites. Organic matter between the microcrystallites would provide the cohesive element for forming the larger composite crystallites that make up the outer shell of the otoconia. As shown in the micrograph of the mineral layer (Fig. 6), organic matter can only rarely be recognized at what appears to be the boundaries of individual crystallites or of small composites thereof. This may imply that proteins or any organic matter present in the mineral matrix are not sufficiently organized for visual detection. In fact, no protein aggregates are visible in the replicas of the fracture faces of the crystalline structure of the aragonitic otoconia of the frog despite the fact that it is presumed to contain as much as 2–11.5% protein (Pote and Ross, 1991; Pote *et al.*, 1993b).

It is not clear what the role of the core is in the formation of the calcitic otoconia, since no core structure is visible in the fractured aragonitic otoconia of the frog (Kurc *et al.*, 1999). The fact that the core has a contour similar to that of the entire otoconium suggests that it may be involved in the mineralization of the outer shell, reinforcing previous interpretations of controlled mineralization of biominerals (Mann *et al.*, 1983; Addadi *et al.*, 1989; Falimi *et al.*, 1996; Khan, 1997). In this context it is interesting that the calcitic otoconia contain pores that would allow the endolymphatic fluid to have direct access to the interior of the otoconia. This suggests that mineralization, growth, and renewal are not limited to the surface of the otoconia.

Without knowing how otoconia develop it is difficult to predict how the orientation of the cortical crystallites is affected by the core matrix which for the most part appears isotropic in organization. However, the outermost layer of the core matrix, which forms regular radial bridges to the outer shell (see Fig. 5c), may function as the organizing element for crystallite growth and orientation, thus reinforcing previous interpretations of controlled mineralization of otoconia and other biominerals (Lowenstam, 1981; Falimi *et al.*, 1996).

In addition to contributing to a basic understanding of vestibular structure, these data may form the basis for future studies of vestibular pathologies. Many of the genetic abnormalities that lead to vestibular deficiencies specifically affect otoconia structure, such as the formation of giant otoconia in the tilted mice (Ornitz *et al.*, 1998; Wang *et al.*, 1998). Freeze-etching studies of the otoconia in such mice should provide valuable information necessary in understanding otoconial malformations in genetic and acquired conditions of vestibular deficiencies.

We thank Jorgen Fex and Ronald Petralia for critical comments on the manuscript. This work was partially supported by FINEP, Pronex, and CNPq.

REFERENCES

Addadi, L., Berman, A., Oldak, J. M., and Weiner, S. (1989) Structural and stereochemical relations between acidic macromolecules of organic matrices and crystals, *Connect. Tissue Res.* **21,** 127–134.

Arima, T., Lim, D. J., Kawaguchi, H., Shibata, Y., and Uemura, T. (1990) An ultrastructural study of the guinea pig tectorial membrane 'type A' protofibril, *Hear. Res.* **46,** 289–292.

Carlstro¨m, D. (1963) A crystallographic study of vertebrate otoliths, *Biol. Bull.* **125,** 441–463.

Eatock, R. A., Corey, D. P., and Hudspeth, J. (1987) Adaptation of mechanoelectrical transduction in hair cells of the bull-frog's sacculus, *J. Neurosci.* **7,** 28221–2836.

Falimi, G., Albeck, S., Weiner, S., and Addadi, L. (1996) Control of aragonite or calcite polymorphism by mollusk shell macromolecules, *Science* **271,** 67–69.

Fermin, C. D., Lychakov, D., Campos, A., Hara, H., Sondag, E., Jones, T., Jones, S., Taylor, M., Meza-Ruiz, G., and Martin, D. S. (1998) Otoconia biogenesis, phylogeny, composition and functional attributes, *Histol. Histopathol.* **13,** 1103–1154.

Gauldie, R. W. (1993) Polymorphic crystalline structure of fish otoliths, *J. Morphol.* **218,** 1–28.

Howard, J., and Hudspeth, A. J. (1987) Mechanical relaxation of the hair bundle mediates adaptation in mechanoelectrical transduction by bullfrog's saccular hair cell, *Proc. Natl. Acad. Sci. USA* **84,** 3064–3068.

Heuser, J. E. (1983) Procedure for freeze-drying molecules adsorbed to mica flakes, *J. Mol. Biol.* **169,** 155–195.

Heuser, J. E., Reese, T. S., Jan, L. Y., Jan, Y. N., Dennis, M. J., and Evans, L. (1979) Synaptic vesicle exocytosis captured by quick-freezing and correlated with quantal transmitter release, *J. Cell Biol.* **81,** 275–300.

Kachar, B., Parakkal, M., and Fex, J. (1990) Structural basis for mechanical transduction in the frog vestibular sensory apparatus: I. The otolithic membrane, *Hear. Res.* **45,** 179–190.

Khan, S. R. (1997) Interactions between stone-forming calcitic crystals and macromolecules, *Urol. Int.* **59,** 59–71.

Kurc, M., Farina, M., Lins, U., and Kachar, B. (1999) Structural basis for mechanical transduction in the frog vestibular sensory apparatus: III The organization of the otoconial mass, *Hear. Res.* **131,** 11–21.

Lim, D. J. (1984) The development and structure of the otoconia, *in* Friedmann, I., and Ballantyne, I. (Eds.), Ultrastructural Atlas of the Inner Ear, pp. 245–269, Butterworths, London.

Lowenstam, H. A. (1981) Minerals formed by organisms, *Science* **211,** 1126–1131.

Mann, S., Parker, S. B., Ross, M. D., Skarnulis, A. J., and Williams, R. J. (1983) The ultrastructure of the calcium carbonate balance organs of the inner ear: An ultra-high resolution electron microscopy study, *Proc. R. Soc. London Biol. Sci.* **218,** 415–424.

Marmo, F., Balsamo, G., and Franco, E. (1983) Calcite in the statoconia of amphibians: a detailed analysis in the frog *Rana esculenta*, *Cell Tissue Res.* **233,** 35–43.

Nakai, Y., Masutani, H., Kato, A., and Sugiyama, T. (1996) Observation of the otolithic membrane by low-vacuum scanning electron microscopy, *J. Oto-Rhino-Laryngol.* **58,** 9–12.

Oliveira, A., Farina, M., Ludka, M. I. P., and Kachar, B. (1996) Vaterite, calcite and aragonite in the otoliths of three species of piranha (*Characiformes: Characidae*), *Naturwissenschaften* **83,** 133–135.

Ornitz, D. M., Bohne, B. A., Thalmann, I., Harding, G. W., and Thalmann, R. (1998) Otoconial agenesis in *tilted* mutant mice, *Hear. Res.* **122,** 60–70.

Pote, K. G., Hauer III, C. R., Michel, H., Shabanowitz, J., Hunt, D. F., and Kretsinger, R. H. (1993a) Otoconin-22, the major protein of aragonitic frog otoconia, is a homologue of phospholipase A2, *Biochemistry* **32,** 5017–5024.

Pote, K. G., Weber, C. H., and Kretsinger, R. H. (1993b) Inferred protein content and distribution from density measurements of calcitic and aragonitic otoconia, *Hear. Res.* **66,** 225–232.

Pote, K. G., and Ross, M. D. (1986) Ultrastructural morphology and protein content of the internal organic material of rat otoconia, *J. Ultrastruct. Mol. Struct. Res.* **95,** 61–70.

Pote, K. G., and Ross, M. D. (1991) Each otoconia polymorph has a protein unique to that polymorph, *Comp. Biochem. Physiol. B* **98,** 287–295.

Ross, M. D., Komorowski, T. E., Donovan, K. M., and Pote, K. G. (1987) The suprastructure of the saccular macula, *Acta Otolaryngol.* **103,** 56–63.

Ross, M. D., and Pote, K. G. (1984) Some properties of otoconia, *Philos. Trans. R. Soc. London B Biol. Sci.* **304,** 445–452.

Salt, A. N., Inamura, N., Thalmann, R., and Vora, A. (1989) Calcium gradients in inner ear endolymph, *Am. J. Otolaryngol.* **10,** 371–375.

Steyger, P. S., and Wiederhold, M. L. (1995) Visualization of newt aragonitic otoconial matrices using transmission electron microscopy, *Hear. Res.* **92,** 184–191.

Steyger, P. S., Wiederhold, M. L., and Batten, J. (1995) The morphogenic features of otoconia during larval development of *Cynops pyrrhogaster*, the Japanese red-bellied newt, *Hear. Res.* **84,** 61–71.

Wang, Y., Kowalski, P. E., Thalmann, I., Ornitz, D. M., Mager, D. L., and Thalmann, R. (1998) Otoconin-90, the mammalian otoconial matrix protein, contains two domains of homology to secretory phosphilipase A_2, *Proc. Natl. Acad. Sci. USA* **95,** 15350–15350.